

# CBERS-4/MUX automatic detection of clouds and cloud shadows using decision trees

Rennan de Freitas Bezerra Marujo<sup>1</sup>  
Leila Maria Garcia Fonseca<sup>1</sup>  
Thales Sehn Körting<sup>1</sup>  
Rafael Duarte Coelho dos Santos<sup>1</sup>  
Hugo do Nascimento Bendini<sup>1</sup>

<sup>1</sup> Instituto Nacional de Pesquisas Espaciais – INPE  
Caixa Postal 515 – 12245-970 – São José dos Campos - SP, Brasil  
{rennan.marujo, leila.fonseca, thales.korting, rafael.santos, hugo.bendini}@inpe.br

**Abstract.** Cloud contamination can compromise surface observation on satellite images and impossibility land cover and land use mapping, due to their high reflectance. Similarly, cloud shadows can darken the image or be confused with water, making it harder to differentiate targets. This paper aims at evaluating an automatic cloud and cloud shadow detection method using decision tree classifier for CBERS-4 (China Brazil Earth Resources Satellite) MUX (Multispectral Camera) camera. In relation to the features used in the classification process, 3 methods were tested to classify 10 images of CBERS-4 MUX camera. The first one used spectral information and spectral indices, such as NDVI, WI and HOT; the second one added shape attributes in the feature set, and the third one added texture attributes. The classification process considered 3 classes: cloud, cloud shadow and cloud-free, which were validated using visually interpreted images. The results presented an overall accuracy of about 92.98%. The accuracy for the cloud detection was 0.91, while for the cloud shadow the classification accuracy was 0.67. These results point out that for sensors that has only visible and near infrared spectral bands, like CBERS-4/MUX, the NDVI, WI and HOT spectral indices are relevant for cloud detection. On the other hand, for cloud shadow detection it is necessary to explore other features capable to discriminate it from dark objects in the images.

**Keywords:** remote sensing, cloud detection, CBERS-4 .

## 1. Introduction

Optical remote sensing has become a widely used technology for Earth observation, although it is vulnerable to clouds, since clouds and cloud shadows affect the radiometric response of the surface (JENSEN, 2007), reducing observed area. To applications, such as, agricultural and forest fire detection for example, it is important to detect clouds and cloud shadows so that they don't interfere in the analysis.

The white color appearance of clouds in the satellite images, is determined by the additive effect of all wavelengths of the visible spectrum (POLIDORIO et al., 2005). Detecting cloud and cloud shadows based exclusively through sensor color (spectral response), usually fails on scenes that present water bodies and exposed soil, because the low reflectance on water bodies result in similar spectral characteristics to areas affected by shadows and the high reflectance on exposed soil may present similar behavior as exhibited by clouds (ABREU et al., 2013).

Song and Civco (2002) proposed a method to detect clouds and cloud shadows on Landsat-5/TM based on changing detection using two images of the same location with different dates. They observed that the blue and near infrared (NIR) bands were spectrally suitable for clouds and cloud shadows detection respectively and empirically threshold values in each band to isolate these classes. This was accomplished by using two images, one containing clouds and another without clouds. The differences between the images were highlighted allowing to identify the regions with clouds or cloud shadows.

Recent methods such as *fmask* algorithm (ZHU; WOODCOCK, 2012; ZHU; WANG; WOODCOCK, 2015), uses Top of Atmosphere (TOA) reflectance and Brightness Temperature as inputs. USGS (United States Geological Survey) uses this method as standard cloud mask for Landsat-7 and an enhanced version of it to Landsat-8 (USGS, 2015). *Fmask* firstly separates Potential Cloud Pixels and clear-sky pixels. Then, the thermal bands (normalized temperature probability) are used alongside with the spectral variability probability, and brightness probability to produce a probability mask for clouds over land and water separately. This probability mask for clouds is combined with the Potential Cloud Pixels and a potential cloud layer is derived (ZHU; WOODCOCK, 2012; ZHU; WANG; WOODCOCK, 2015). Similarly to Song and Civco (2002), Zhu and Woodcock (2012) used a dark pixels mask extracted from the NIR band, but in this case it is confirmed using the view angle of the satellite sensor and the illuminating angle to predict possible cloud shadow locations and select the one that has the maximum similarity with the potential cloud shadow mask.

Thinking on sensors that doesn't act in the thermal wavelengths, Silva and Liporace (2016) proposed an adaption on the *fmask* algorithm (ZHU; WOODCOCK, 2012; ZHU; WANG; WOODCOCK, 2015) to ensure the method to automatically detect cloud and cloud shadow using visible and near infrared spectrum. Originally the methodology was proposed to be used on Amazonia-1/AWFI. To identify clouds, the authors used a 3 indices threshold: NDVI, WI and HOT, while to detect cloud shadows, they integrated a dark pixels mask, obtained with green and NIR bands. The authors also used a water mask, using NIR and NDVI and a difference image resulted from comparison to a reference image ideally free cloud and perfectly registered.

Given the cloud mask importance and the difficulties to obtain this product, this study aims for a cloud and cloud shadow detection method that can be applied to CBERS-4 (China Brazil Earth Resources Satellite) MUX (Multispectral Camera) sensor and other sensors that uses only the visible and Near Infrared (NIR) bands. In order to do that, we adapted the Silva and Liporace (2016) method to automatically find the threshold intervals through a decision tree, and tried to improve it by also using shape and texture attributes to detect cloud and cloud shadow.

## 2. Methodology

The study area is situated in the southeast of Brazil, near São Paulo and Minas Gerais states frontier, being the predominant activity in it the agriculture. A total of 10 CBERS-4/MUX (CBERS WRS Path/Row 155/124) scenes, covering the period from March 1st to July 7th (2016), were freely acquired from INPE's (Brazilian National Institute for Space Research) image catalog. As shown on Table 1, the images have four spectral bands: blue, green, red and Near Infrared with 20 meters of spatial resolution and a revisit period of 26 days. Those images digital number values were converted to TOA reflectance following Pinto et al. (2016) recommendations.

All image were segmented using multiresolution segmentation (BAATZ; SCHÄPE, 2000). Segmentation parameters were empirically defined as: 0.8 on color; 0.5 on compactness and 30 on scale, since the human eye is a strong and experienced evaluator of segmentation techniques (GAMANYA; De Maeyer; De Dapper, 2007). The segmentation resulted in approximately 30000 segments per image, which were used to extract a total of 76 different attributes.

The methodology can be seen in Figure 1. The data mining process was done using the R language WEKA's library (HALL et al., 2009) and visually interpreted images as reference. The invalid instances were removed from the training set and the valid ones inputted in C4.5 (QUINLAN, 1993) WEKA's implementation (also named J48) (HALL et al., 2009). The classifications aimed three classes: cloud, cloud shadow and cloud-free objects, using a 10 fold cross-validation, a minimum number of objects per leaf equal to 150. The first classification

Characteristic	CBERS-4/MUX
Technique	Pushbroom
Altitude	778 km
Swath Width	120 km
Field of View (FOV)	±4°
Spectral Bands (nm)	450–520 (Blue)
	520–590 (Green)
	630–690 (Red)
	770–890 (NIR)
Spatial Resolution	20 m
Temporal Resolution	26 days
Radiometric Resolution	8 bits

Table 1: Summary of the MUX on-board CBERS-4 characteristics.  
Source: adapted from Epiphonio (2011).

used exclusively spectral information (band means, standard deviation) and the indices NDVI, WI and HOT; the second classification also included shape attributes; and the third also includes texture attributes as Table 2 describes.

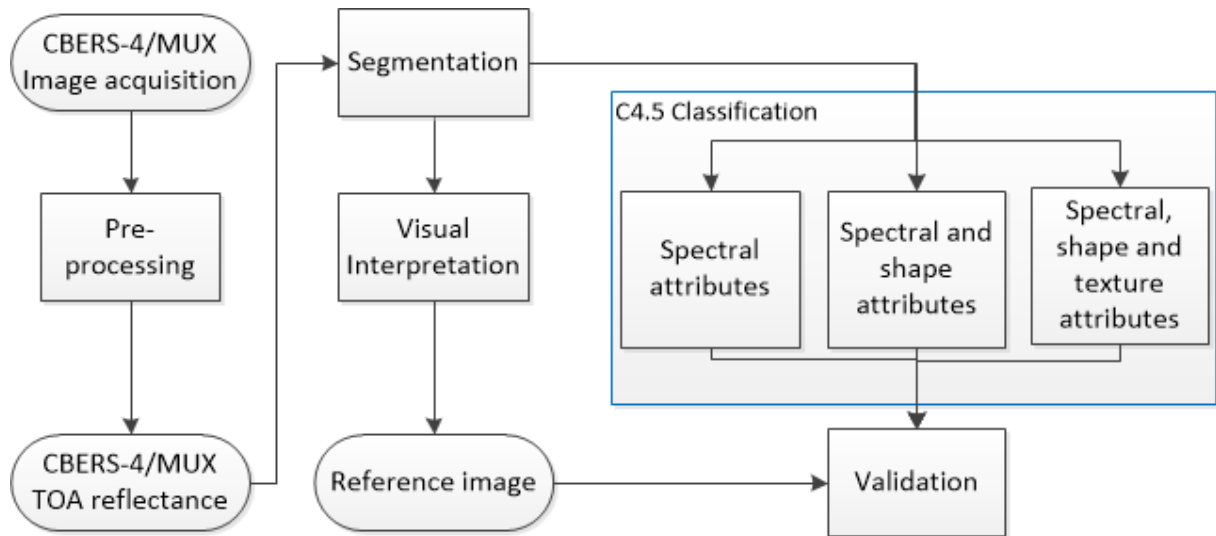


Figure 1: Methodology diagram used to classify Cloud, Cloud Shadow and Cloud free areas in CBERS-4/MUX images through decision tree (C4.5) algorithm.

The NDVI (Normalized difference vegetation index) (ROUSE et al., 1974) is a vegetation index to analyse vegetative vigor which can be acquired by band arithmetics using the red and near infra-red bands, as shown in equation 1.

$$NDVI = \frac{NIR - Red}{NIR + Red} \quad (1)$$

where *NIR* is the Near Infra-red band and *Red* is the red band. In Landsat-8/OLI, the red band and near infra-red are band-4 and band-5, respectively.

The Whiteness Index is an index, originally proposed by Gómez-Chova et al. (2007), used to verify if a region is “white” enough to be a cloud. In order to calculate the WI, the band mean

Classification	Attributes
First Classification	Spectral indices (NDVI, WI, M, HOT)
	Spectral bands (Blue, Green, Red and NIR)
	Standard deviation (Blue, Green, Red and NIR)
Second Classification	First Classification attributes + Shape attributes (Asymmetry, Border Index, Compactness, Density, Elliptic Fit, Length, Main direction, Rectangularity, Roundness, Shape index, Volume, Width)
	Second Classification attributes + Texture attributes (Angular second moment, Contrast, Correlation, Dissimilarity, Entropy, Homogeneity, Mean, Standard deviation, Contrast, Correlation)

Table 2: Summary of used attributes in three classifications; the first classification using spectral band means, standard deviation and spectral indices; the second classification also including shape attributes and the third also including texture attributes.

value is needed as shown on equation 2. After computing  $M$ , the WI can be obtained through equation 3.

$$M = 0.25 \cdot B_1 + 0.375 \cdot B_2 + 0.375 \cdot B_3 \quad (2)$$

where  $B_1$  is the blue band,  $B_2$  is the green band and  $B_3$  is the red band, respectively.

$$WI = \sum_{i=1}^3 \left| \frac{(B_i - M)}{M} \right| \quad (3)$$

where  $M$  is the modified mean band value obtained through equation 2 and  $B_i$  are the visible bands, respectively.

The Haze Optimized Transformation (HOT) is an index, originally proposed by Zhang, Guindon and Cihlar (2002), used to detect and characterize haze and cloud spatial distributions originally in Landsat scenes and it is given as shown on equation 4.

$$HOT = B_1 - 0.45 \cdot B_3 - 0.08 \quad (4)$$

where  $B_1$  and  $B_3$  are the blue and red band, respectively.

The spectral mean attributes is calculated through a simple mean using all pixels contained in the same segment for each band; Similarly, the standard deviation of a segment consists in the mean standard deviation of all pixels contained in the same segment for each band.

The shape attributes used were: length and width, which can be extracted using the segment bounding box; asymmetry, that reflects the more longish a segment is; the shape index, that is the border length of the segment divided by four times the square root of its area and similarly is the border Index, but instead of a square it uses the smallest rectangle; the compactness, that is similar to border index, but instead of border length it uses the area; the density, that expresses the area covered by the segment divided by its radius; the elliptic fit, that is the filled percentage of the segment in comparison to an ellipse; the rectangularity, that is the difference of enclosing/enclosed rectangle and similarly the roundness, but using an enclosing/enclosed ellipse and for last the main direction, that represents the direction eigenvector belonging to the larger of the two eigenvalues derived from the covariance matrix of the spatial distribution of the segment (DEFINIENS, 2007).

Textures are statistical metrics that measures the pixels spreading variation in a segment (HARALICK; SHANMUGAM; DINSTEIN, 1973) and in this study were used the Haralick, Shanmugam and Dinstein (1973) Gray Level Cooccurrence Matrices (GLCM) and Gray Level Difference Vector (GLDV): Angular second moment, Contrast, Correlation, Dissimilarity, Entropy, Homogeneity, Mean, Standard deviation, Contrast and Correlation.

### 3. Results and Discussions

The use of image segmentation before classification successfully grouped similar pixels, not being necessary a post processing, as in Silva and Liporace (2016) and others pixel based approaches, to correct salt and pepper effects (BLASCHKE et al., 2000).

At the classification phase, the insertion of the shape and texture attributes, did not considerable increased the overall accuracy when identifying cloud, cloud shadows and cloud-free regions using C4.5 algorithm, as it was expected, since shadows don't have any particular texture and clouds textures varies depending on the cloud type and concentration. In fact, the overall accuracy remained almost the same, as can be seen in Table 3. The lower accuracies obtained (84.13%, 86.97% and 87.00%) were found on the most clouded images.

The use of all the input images, to generate an overall classification tree, resulted on the rule tree shown on Figure 2. The right branch of the tree, after blue band mean value, corroborates Silva and Liporace (2016) method to cloud detection, using the HOT, NDVI AND WI indices, resulting in a precision of 0.91 to the cloud class, as shown on Table 4. The left branch of the tree separates cloud shadow from cloud-free regions, through the blue band mean value, what can supposedly be interpreted as the dark region mask used by Silva and Liporace (2016). Those attributes were efficient to detect clouds in CBERS-4/MUX, although their values can not be generalized, because of the interference caused by the atmosphere, principally in the lower ones as the blue band (JENSEN, 2007). The global accuracy of the classification of the tree showed on Figure 2 was 92.98%, being the lowest precision found to the cloud shadow class (0.67), demonstrating that this class is not fully separable using the visible and near infrared bands, probably being mixed with water class, and surface shadows as pointed by Abreu et al. (2013), Polidorio et al. (2005), Silva and Liporace (2016), Song and Civco (2002), Zhang, Guindon and Cihlar (2002) and can be visually confirmed in image 3.

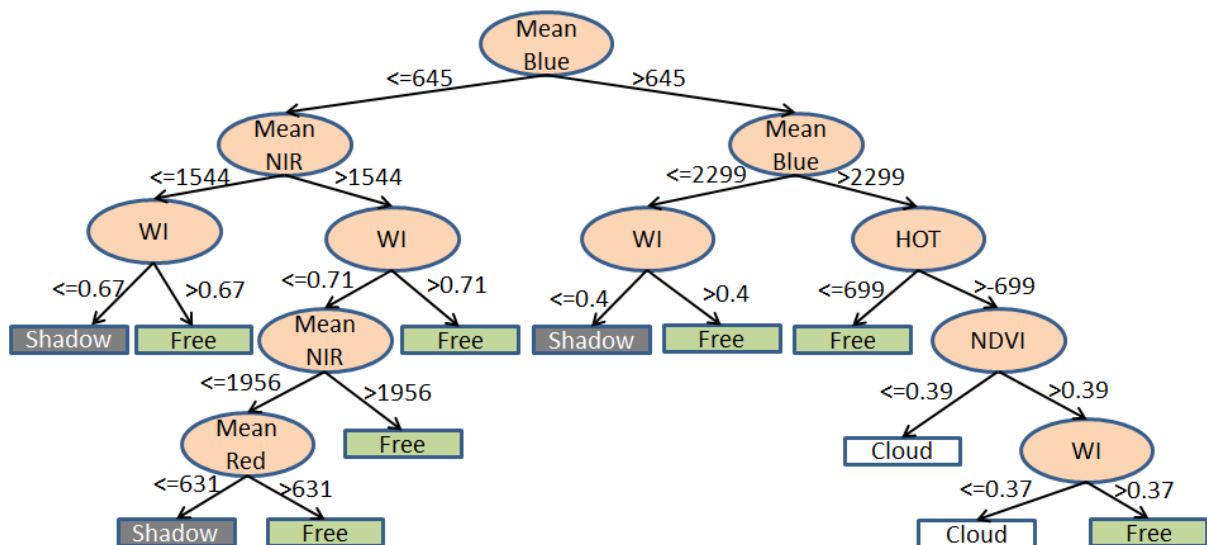


Figure 2: CBERS-4/MUX (Path/Row 155/124) classification rule tree to cloud, cloud shadow and cloud-free segments.

CBERS-4/MUX image date	Classification 1 accuracy (%)	Classification 2 accuracy (%)	Classification 3 accuracy (%)
2016/07/07	93.16	93.18	93.19
2016/04/20	99.70	99.70	99.70
2016/02/02	98.76	98.76	98.76
2015/12/12	84.13	84.41	84.28
2015/11/16	87.00	86.83	87.29
2015/09/25	86.97	86.98	87.17
2015/08/30	99.98	99.98	99.98
2015/08/04	99.10	99.10	99.10

Table 3: Summary of the CBERS-4/MUX (Path/Row 155/124) accuracies using spectral attributes and spectral indices (Classification 1), including shape attributes (Classification 2) and including texture attributes (Classification 3).

Classification	Cloud precision	Cloud shadow precision	Cloud-free precision	Accuracy (%)
Classification 1	0.915	0.670	0.946	92.9802

Table 4: Summary of the CBERS-4/MUX (Path/Row 155/124) class precisions and accuracy using spectral attributes on images from March 1st to July 7th (2016).

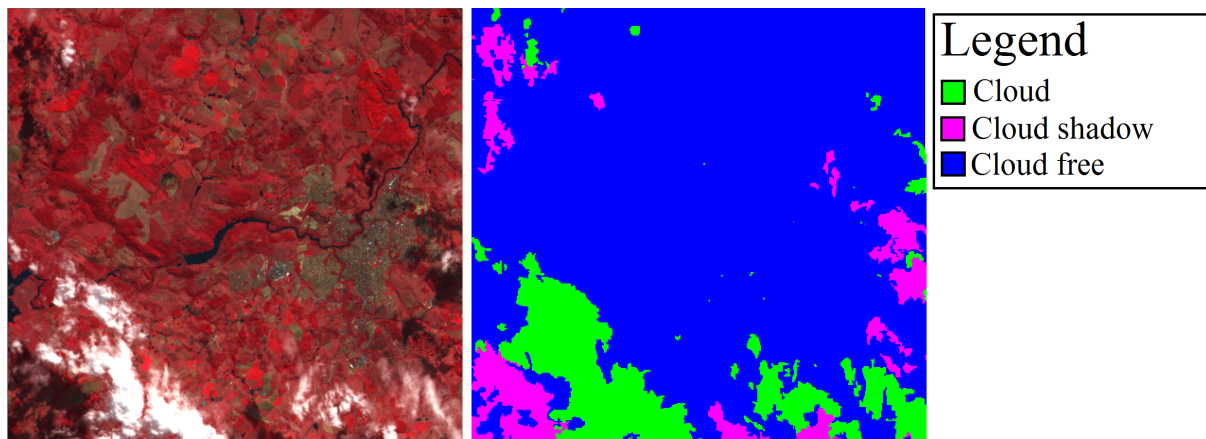


Figure 3: CBERS-4/MUX (Path/Row 155/124) subset in false color (R:NIR, G:Red, B:Green) and classification of Cloud, Cloud shadow and cloud free areas using decision tree (C4.5) algorithm.

#### 4. Conclusions and Future Work

In this work we tested a methodology for cloud and cloud shadow detection on CBERS-4/MUX, a sensor capable of acquiring images exclusively on visible and near infra red wavelengths. The tests to evaluate spectral, shape and texture attributes were done using the C4.5 decision tree classifier in each image and posteriorly on all the data.

- The decision tree method provided visually interpretative rules to separate cloud, cloud shadow and cloud-free regions;
- The NDVI, WI and HOT spectral indices provide useful information in cloud detection, to sensors that does not have thermal or blue coastal bands, as is the case of CBERS-4/MUX;
- The low precision found on cloud shadow indicates that more robust methods are required to separate it instead of spectral values directly;

Future works are focused on using previous know areas to map water regions and context information to associate clouds with its cloud shadows, as demonstrate by Silva and Liporace (2016), Zhu and Woodcock (2012), Zhu, Wang and Woodcock (2015).

#### 5. Acknowledgments

The authors would like to thank the Brazilian National Institute for Space Research (INPE) and FAPESP (Project # 2014/08398-6 and Process # 2016/08719-2), São Paulo Research Foundation for funding this research.

#### References

- ABREU, E. S. et al. "Cloud Detection Tool" – Uma ferramenta para a detecção de nuvens e sombras em imagens de satélite. In: *Simpósio Brasileiro de Sensoriamento Remoto*. Foz do Iguaçu: [s.n.], 2013. v. 16, n. 16, p. 4234–4241.
- BAATZ, M.; SCHÄPE, A. Multiresolution segmentation: an optimization approach for high quality multi-scale image segmentation. In: *Angewandte geographische Informationsverarbeitung*. [s.n.], 2000. p. 6. Disponível em: <<http://scholar.google.com/scholar?hl=en&btnG=Search&q=intitle:Multiresolution+Segmentation+:+an+optimization+approach+for+high+quality+multi-scale+image+segmentation#0>>.
- BLASCHKE, T. et al. Object-Oriented Image Processing in an Integrated GIS / Remote Sensing Environment and Perspectives for Environmental Applications. *Umweltinformation für Planung, Politik und Öffentlichkeit / Environmental Information for Planning, Politics and the Public*, n. 1995, p. 555–570, 2000.
- DEFINIENS. *Definiens developer 7 reference book*. [S.l.], 2007. 195 p. Disponível em: <<http://scholar.google.com/scholar?hl=en&btnG=Search&q=intitle:Definiens+Developer+7+Reference+Book#0>>.
- EPIPHANIO, J. C. N. CBERS-3/4: características e potencialidades José. In: *Simpósio Brasileiro de Sensoriamento Remoto*. Curitiba: [s.n.], 2011. v. 15, p. 9009–9016. Disponível em: <<http://www.dsr.inpe.br/sbsr2011/files/p1222.pdf>>.
- GAMANYA, R.; De Maeyer, P.; De Dapper, M. An automated satellite image classification design using object-oriented segmentation algorithms: A move towards standardization. *Expert Systems with Applications*, v. 32, n. 2, p. 616–624, 2007. ISSN 09574174.

GÓMEZ-CHOVA, L. et al. Cloud-screening algorithm for ENVISAT/MERIS multispectral images. *IEEE Transactions on Geoscience and Remote Sensing*, v. 45, n. 12, p. 4105–4118, 2007. ISSN 01962892.

HALL, M. et al. The WEKA data mining software. *ACM SIGKDD Explorations Newsletter*, Association for Computing Machinery (ACM), v. 11, n. 1, p. 10, nov 2009. Disponível em: <<http://dx.doi.org/10.1145/1656274.1656278>>.

HARALICK, R. M.; SHANMUGAM, K.; DINSTEN, I. Textural features for image classification. *IEEE Transactions on Systems, Man, and Cybernetics*, Institute of Electrical and Electronics Engineers (IEEE), v. 3, n. 6, p. 610–621, nov 1973. Disponível em: <<http://dx.doi.org/10.1109/tsmc.1973.4309314>>.

JENSEN, J. R. *Remote Sensing of the Environment: An Earth Resource Perspective*. 2. ed. Upper Saddle River: Prentice Hall, 2007. 592 p.

PINTO, C. et al. First in-Flight Radiometric Calibration of MUX and WFI on-Board CBERS-4. *Remote Sensing*, v. 8, n. 5, p. 405, 2016. ISSN 2072-4292. Disponível em: <<http://www.mdpi.com/2072-4292/8/5/405>>.

POLIDORIO, A. M. et al. Detecção automática de sombras e nuvens em imagens CBERS e Landsat 7 ETM. In: *Simpósio Brasileiro de Sensoriamento Remoto*. Goiânia: [s.n.], 2005. p. 4233–4240.

QUINLAN, J. C4. 5: programs for machine learning. *Machine Learning*, v. 240, p. 302, 1993. ISSN 08856125.

ROUSE, J. W. et al. Monitoring vegetation systems in the Great Plains with ERTS. In: *Proceedings...* [S.l.: s.n.], 1974. p. 309–317.

SILVA, M. A. O. da; LIPORACE, F. d. S. Detecção automática de nuvem e sombra de nuvem em imagens de sensoriamento remoto. *Boletim de Ciências Geodésicas*, v. 22, n. 2, p. 369–388, 2016. ISSN 1982-2170.

SONG, M.; CIVCO, D. L. A knowledge-based approach for reducing cloud and shadow. In: *ASPRS-ACSM Annual Conference and FIG XXII Congress*. Washington: [s.n.], 2002. v. 22, p. 1–7. Disponível em: <[http://clear.uconn.edu/publications/research/tech\\_papers/Song\\_Civco\\_ASPRS2002.pdf](http://clear.uconn.edu/publications/research/tech_papers/Song_Civco_ASPRS2002.pdf)>.

USGS. *Product Guide*. [S.l.], 2015. 27 p.

ZHANG, Y.; GUINDON, B.; CIHLAR, J. An image transform to characterize and compensate for spatial variations in thin cloud contamination of Landsat images. *Remote Sensing of Environment*, v. 82, n. 2-3, p. 173–187, 2002. ISSN 00344257.

ZHU, Z.; WANG, S.; WOODCOCK, C. E. Improvement and expansion of the fmask algorithm: cloud, cloud shadow, and snow detection for landsats 4–7, 8, and sentinel 2 images. *Remote Sensing of Environment*, v. 159, p. 269 – 277, 2015. ISSN 0034-4257. Disponível em: <<http://www.sciencedirect.com/science/article/pii/S0034425714005069>>.

ZHU, Z.; WOODCOCK, C. E. Object-based cloud and cloud shadow detection in landsat imagery. *Remote Sensing of Environment*, v. 118, p. 83 – 94, 2012. ISSN 0034-4257. Disponível em: <<http://www.sciencedirect.com/science/article/pii/S0034425711003853>>.